J Mater Sci (2013) 48:4801–4805
DOI 10.1007/s10853-013-7195-y

NANOSTRUCTURED MATERIALS

High-temperature oxidation resistance of ultrafine-grained 14 %Cr ODS ferritic steel

Zbigniew Oksiuta

Received: 30 November 2012 / Accepted: 24 January 2013 / Published online: 6 February 2013

Abstract The long-term oxidation resistance of the Fe–14Cr–2W–0.3Ti–0.3Y_2O_3 oxide dispersion strengthened reduced activation ferritic steel was investigated. The results of the long-term oxidation at 750 °C for 10000 h in air revealed that the weight gain of the ODS ferritic steel was exceptionally low ($<3.5 \times 10^{-3}$ g/cm^{-2}) and that the long-term oxidation rate follows the parabolic law. The parabolic rate constant, which was calculated from the mass change during the ageing process was equal to 2.0×10^{-9} g^2/cm^4 h. The scanning electron microscopy (SEM) observations of the cross section of the specimen after being aged for 10000 h revealed an oxide scale with the non-uniform thickness ranging from 2.0 to 5.0 μm enriched with Cr–Mn oxide. On the contrary to the SEM observations of the ODS steel scale following the annealing process at 1350 °C, it was revealed that the material had a multi-layer scale with the thickness equal to ~20 μm. The outer layer, with the approximate thickness of 15 μm, was mainly composed of 30Fe–22Cr–8W–2Si–38O (in wt%), whereas the inner part of the layer was predominantly made of 76Fe–14Cr–2W–10O.

Introduction

The oxide dispersion strengthened (ODS) reduced activation ferritic (RAF) steels as a structural constituent in future fusion reactors will have to withstand high temperatures, high heat flux as well as neutron irradiation conditions [1]. Due to its unique microstructure (ultrafine grains containing oxide nanoparticles), the ODS steel has not only excellent high-temperature strength but also thermal stability. However, at a certain temperature, the grain and nanoparticle coarsening effects are expected (this problem is discussed elsewhere) [2]. On the other hand, taking into consideration the fact that the operating temperature window for the ODS ferritic steels is expected to be in the range between 600 and 800 °C, the material will also be subject to the high-temperature oxidation at extended service time [3]. Although the high-temperature oxidation process for the ODS RAF steel has not been widely described in the literature yet, it is noteworthy to find out more about a protective oxide layer that can be formed on the ODS RAF steel during various times as well as temperature treatment conditions.

The ODS RAF steel is commonly manufactured by means of the powder metallurgy (PM) route, which consists of mechanical alloying and further powder consolidation implementing the hot isostatic pressing (HIP) and/or hot extrusion (HE) methods [4]. The high-speed hydrostatic extrusion (HSHE) process is one of the alternative methods, which ensures unique and exceptional properties of a material [5, 6]. This is due to the fact that high hydrostatic pressure of the fluid obtained during the extrusion process reduces the friction between the billet and the container surface. Moreover, during the aforementioned circumstance, both comprehensive as well as shear forces are generated. [7]. On the other hand, since elongated towards the extrusion direction microstructures (texture) and anisotropic mechanical properties of material are observed perpendicularly to the extrusion direction, [8] this technique is commonly applied in the production of complex cross sections as well as rod (tube) type of materials.

Z. Oksiuta (✉)
Mechanical Department, Bialystok University of Technology, Wiejska 45c, 15-351 Bialystok, Poland
e-mail: z.oksiuta@pb.edu.pl

In this work, the ultrafine-grained ODS RAF steel was produced through the process of powder metallurgy route followed by the HIP and HSHE processes. The main goal of this work is to acquire more information about a protective oxide layer that can be formed on the ODS RAF steel during various times as well as temperature treatment conditions. Hence, the following work presents comprehensive information about the oxidation mechanism and resistance of the ODS steel.

Experimental procedure

The ODS RAF steel was prepared from a pre-alloyed, argon-atomised Fe–14Cr–2W–0.3Ti (in wt%) powder with 0.3 % of Y_2O_3 nanoparticles by mechanical alloying (MA) in a ball mill under hydrogen atmosphere. The procedure of powder consolidation consisted of canning, vacuum degassing at 450 °C and HIPping at 1150 °C for 3 h followed by the HSHE procedure at 900 °C in order to close the residual porosity and homogenise bimodal grain size microstructure, which was observed after HIPping [9]. Following the hydrostatic extrusion, two kinds of heat treatment were performed: (i) long-term ageing at 750 °C for 10000 h in the atmospheric air and (ii) annealing at 850–1350 °C for 1 h in air, allowing to slowly cool down in the furnace to ambient temperature. Chemical composition of the tested material is summarised in Table 1. Oxidation behaviour of the ODS RAF steel after being subject to ageing at 750 °C for 10000 h in air was determined by a mass gain measurement of the exposed specimens every 1000 h with the help of the analytical balance.

Observations of the oxide layer and linear element distribution following the heat treatments were performed by means of the scanning electron microscopy (SEM) in a type 3000 Hitachi equipped with the electron diffraction spectroscopy (EDS) microprobe and the Hitachi HD2700 Scanning Transmission Electron Microscope (STEM) equipped with the electron energy loss spectroscopy (EELS) detector.

Results and discussion

The results of weight gain and the parabolic rate constant following the long-term ageing process at 750 °C for 10000 h are shown in Fig. 1. Due to the fact that the oxidation rate is both, temperature and time dependent, the diffusion of ions throughout the scale of the steel is the leading rate-controlling oxidation parameter. Thus, the weight gain during the long-term oxidation can be calculated from the equation presented below [10]:

$$(\Delta W)^{1/n} = k_p \cdot t, \quad (1)$$

where ΔW is the weight change of the tested material, t is the exposure time, n is an oxidation exponent describing the time dependence of oxide growth and k_p is the parabolic rate constant.

The mass change measured for the ODS steel after ageing for 10000 h was exceptionally low ($< 3.5 \times 10^{-3}$ g/cm^{-2}). The specific weight gain (related to the surface area of the tested specimens) after 1000 h of ageing was equal to 4.1×10^{-4} g/cm^2. The weight gain compared with the ageing time data is shown in Fig. 1a. It indicates that the oxidation rate follows the steady-state parabolic law [11], and the oxidation exponent n, obtained by fitting the experimental data, was equal to $\sim$0.4. The parabolic rate constant calculated from the mass change during the ageing process was equal to 2.0×10^{-9} g^2/cm^4 h (Fig. 1b). Hence, it emphasises that the ODS RAF steel exhibits outstanding oxidation resistance, similar to the results reported by Hoelzer et al. [12] for the Fe–13Cr ODS ferritic steel.

The aforementioned oxidation behaviour may suggest that the stable and self-protecting oxide scale is formed on the surface of the ODS steel. Thus, the scale of the material after the long-term ageing was observed by means of SEM–EDS (Fig. 2).

SEM observations of the cross section of the specimen after ageing for 10000 h revealed the oxide scale with the non-uniform thickness up to 5.0 μm, as presented in Fig. 2a. SEM–EDS analysis (Fig. 2b) indicated that the scale consisted mainly of Cr–Mn oxide (40Cr–40Mn–6Fe–14O, in wt%) with C and very low Si content and exhibited overall iron depletion. The above findings are not in accordance with the results reported by Kaito et al. [13] for the 9Cr-ODS martensitic steel and the 12Cr-ODS ferritic steel where the thickness of the oxide layer after ageing was uniform and equalled to 20 and 10 mm, respectively. However, it ought to be noted that the authors used dissimilar temperature and time parameters, 650 °C and 2000 h, respectively, and dry air atmosphere, which may explain the discrepancies in the observed layer.

Table 1 Chemical composition of the ODS ferritic steel

Material	Cr	W	Mo	Ti	Mn	Ni	Al	C	N	Si	O	Fe
ODS	13.6	1.9	0.02	0.33	0.38	0.1	0.1	0.06	0.018	0.35	0.17	Bal.

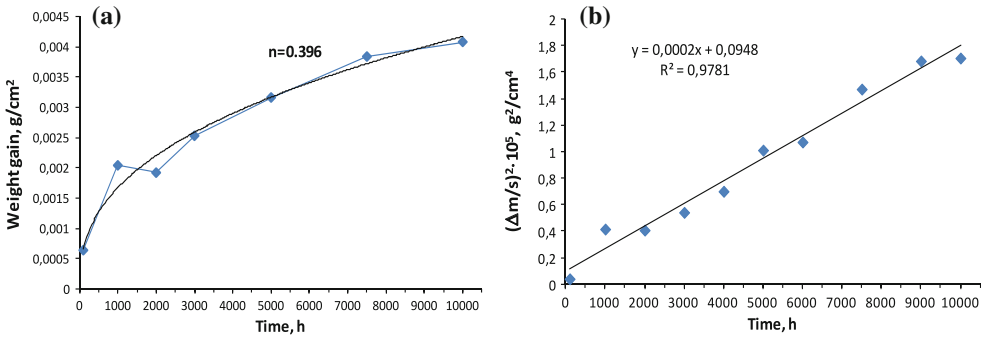

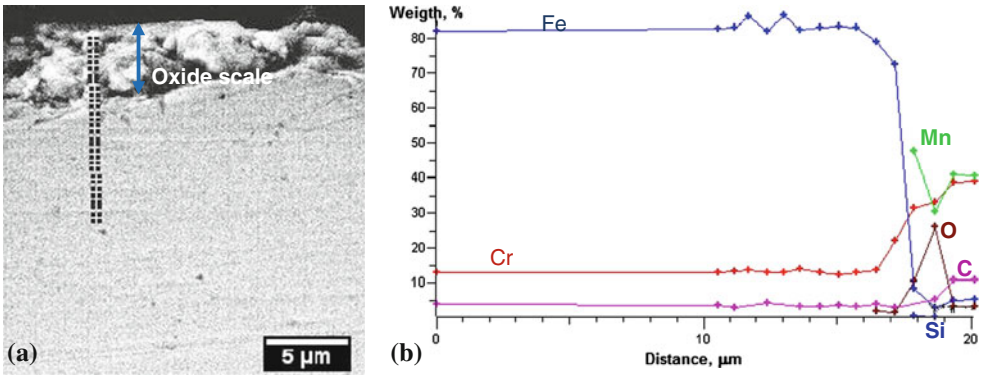

Fig. 1 Weight gain (**a**) and parabolic rate constant data (**b**) as a function of ageing time measured for the ODS ferritic steel after ageing at 750 °C for 10000 h in air

Fig. 2 **a** SEM cross section of the tested specimen and **b** EDS line scan of the ODS RAF steel after ageing at 750 °C for 10000 h in air

Unexpectedly, no W was detected on the oxide scale of tested materials. This shall be regarded as an interesting outcome since the ODS steel has about 2.0 % of *W*, which is five times more than Mn (~0.38 wt%). This may be related to the inhomogeneous distribution of the W element in the mechanically alloyed ODS steel matrix, as well as low coefficient of W diffusion in iron at the ageing temperature. The diffusion coefficient of W in the iron matrix at higher temperatures can be theoretically projected employing the relation proposed by Takemoto et al. [14]. The diffusion coefficient calculated for Tungsten in the bcc iron matrix at 750 °C was equal to $\sim 5.0 \times 10^{-15}$ m^2/s, whereas according to Ollivier-Leduc et al. [15] the diffusion coefficient of Manganese in bcc steel at similar temperature has a higher value ($\sim 2.6 \times 10^{-15}$ m^2/s). This finding undoubtedly underlines that diffusivity of Mn in ferritic steel at the tested temperature conditions, is higher than *W*, and may explain the Mn concentration measured on the surface of the ODS steel oxide layer.

Higher quantity of Mn on the oxide scale of steel was also measured by Jablonski and Alman [16]. Oxide scale rich in Fe–Cr–Mn was formed on the surface of the high-chromium ferritic steel (Fe–22Cr–1Ti–0.5Mn) and tested in the moist air at the temperature of 800 °C for 2000 h. This implies that a small amount of Manganese (~0.4 wt%), present in the matrix of the ODS steel, despite high Cr content (14 %), may form during the long-term heat treatment of the Cr–Mn protective oxide layer, thus confirming that Mn is one of the most effective oxide layers creating an element. In contrary to that, SEM observations revealed that it was not a uniform layer, which in turn highlights the inhomogeneity problem of the ODS RAF steel microstructure.

In order to assess as well as comprehend more about the oxidation resistance of the ODS steel, very high-temperature heat treatment of 1350 °C was applied in air for the duration of one hour. The SEM–EDS images of the specimen's cross section succeeding the annealing process are shown in Fig. 3. Contrary to the long-term ageing process, the ODS RAF steel had a multi-layer uniform oxide scale with the thickness of ~20 µm. The outer layer, with its thickness of approximately of 15 µm, consisted mainly of the 30Fe–22Cr–8W–2Si–38O (in wt%), as it was indicated by the EDS analysis (Fig. 3b). The inner part of the layer, denoted by a darker line with the thickness of ~5 µm, was predominantly composed of the Fe–Cr rich oxide with a lower amount of Tungsten (70Fe–18Cr–2W–10O). Thus, the outer layer was richer in Cr, W and Si and Iron depleted, in comparison with the inner layer. It should be mentioned that Ti and Y elements were not detected by the EDS, which points towards the fact that the aforementioned elements are strongly involved in the formation of Ti–Y–O nanoparticles.

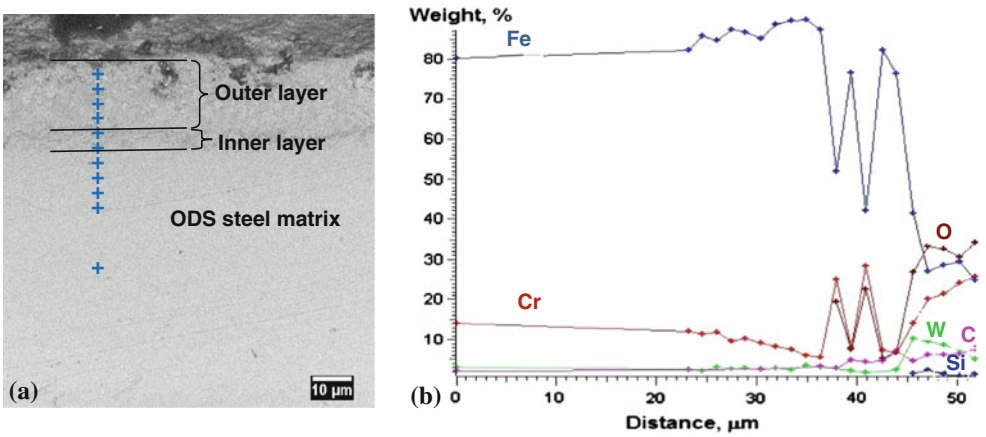

Fig. 3 **a** SEM cross section of the ODS RAF steel after annealing at 1350 °C for 1 h in air. **b** EDS line scan

Interestingly, the outer layer of the material annealed at 1350 °C had approximately 2.0 wt% of Si content, despite relatively low Si content of ~0.30 wt% measured for the ODS RAF steel. Furthermore, in the case of long-term ageing no Mn was detected. Additionally, it should also be recorded that the W element was measured on the cross section of the annealed oxide scale of the steel specimen.

Literature studies reveal that the formation of a silica-rich oxide scale in the high chromium content steels improves their oxidation resistance [17–19]. McDowell and Basu [19] report that the silica layer can provide pathways for rapid Cr diffusion towards the surface. Furthermore, it acts as a diffusion barrier for oxygen migration into steel, thus slowing down the oxidation kinetics.

Taking into account the SEM–EDS analysis of the specimens, which was performed at two different heat treatment conditions, it must be noted that the scales were not similar in thickness, morphology as well as composition (see Fig. 4), which signifies two various mechanisms of the ODS steel oxidation. The lower Cr content measured in the specimen after annealing at 1350 °C was attributed to the volatilization of CrO_3 from the surface of the material, which resulted in greater thickness of the oxide scale. The iron content that was higher by approximately 30 % may also indicate that at 1350 °C, the tight Cr oxide layer was broken, and when the specimen became depleted of Cr, iron oxide was formed rapidly.

Unexpectedly, a high amount of Manganese observed at the cross section of the oxide scale after the long-term ageing is in fact problematic to explain. Usually, ferritic steels with similar Mn and Si element content ~0.5 wt% following the oxidation process exhibit merely a Si-rich oxide scale. This is due to the fact that the free Gibbs energy formation of SiO_2 at 750 °C is more negative than that of MnO, −175 and −150 kcal/mol, respectively [18]. Moreover, according to the literature available, the

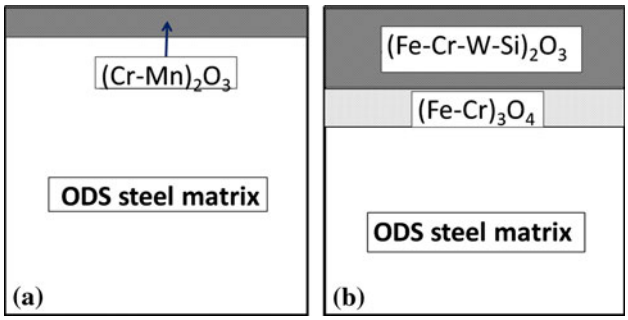

Fig. 4 Schematic illustration of the oxidation effect of the ODS RAF steel performed under various annealing conditions: **a** after ageing at 750 °C for 10000 h and **b** after annealing at 1350 °C for 1 h in air

diffusion coefficient of Mn in ferrite at 800 °C is lower than the diffusion coefficient of Si, 3.2×10^{-15} and 2.6×10^{-15} m^2/s, respectively [16]. However, the diffusion coefficients of Mn and Si in the ODS steel may differ from those described in the literature for conventional ferritic steels obtained by melting and casting. This conclusion originates from an assumption that the ODS RAF steel is a highly work hardened material, with numerous sub-grain boundaries, dislocations, and a great number of point defects, all of which may generate preferential paths for faster diffusion of both elements. Thus, further investigations of the ODS steel should be carried out in order to expand the knowledge regarding the aforementioned effect.

Disparate oxidation mechanisms of the ODS RAF steel after short-term annealing at 1350 °C in contrast to long-term ageing at 750 °C are probably attributed to the Si and W elements detected on the cross section of the oxide scale. These elements at high temperature can diffuse faster into the surface of the ODS steel and form a complex W–Si oxide barrier that according to the literature impedes the outward diffusion of Cr ions and, therefore, slows the growth of scale. At lower ageing temperature, it seems that Mn plays a key role in the oxide scale formation.

Conclusions

In oxidation tests performed in this work, two different oxide scales dependent on time and temperature of heat treatment were observed. The thick, multi-layered chromium-rich (30Fe–22Cr–8W–2Si–38O, in wt%) oxide scale was formed after high-temperature annealing of the steel at 1350 °C. On the other hand, the 5 μm Cr–Mn oxide scale (40Cr–40Mn–6Fe–14O, in wt%) was measured for the material ageing at 750 °C, which in turn was also depleted of iron. The specific weight gain of the material after 10000 h of oxidation demonstrates the parabolic kinetic rate, which emphasises non-homogeneous element distribution in the tested material. Moreover, the finding also indicates that the diffusion rate of the main elements at the temperature of 750 °C in the steel matrix was very low, probably owning to the fact of being strongly impeded by yttria nanoparticles.

Numerous oxidation mechanisms of the ODS RAF steel at 1350 °C in comparison with long-term ageing are probably attributed to the Si and W elements, which were detected on the cross section of the oxide scale. These elements at high annealing temperature can diffuse faster into the surface of the ODS steel and thus create a complex W–Si barrier that according to the literature available slows the growth of scale.

Acknowledgements This work was carried out within the framework of the European Fusion Development Agreement. It was supported by grants from the European Communities within the EURATOM-IPPLM and EURATOM- Confédération Suisse Technical Program and the Polish Ministry of Science and Higher Education.

References

1. de Castro V, Marquis EA, Lozano-Perez S, Pareja R, Jenkins ML (2011) Acta Mater 59:3927
2. Oksiuta Z, Kozikowski P, Lewandowska M, Ohnuma M, Suresh K, Kurzydlowski KJ (2012) J Mat Sci, doi:10.1007/s10853-012-6460-9
3. Hayashi T, Sarosi PM, Schneibel JH, Mills MJ (2008) Acta Mater 6:1407
4. Oksiuta Z, Boehm-Courjault E, Baluc N (2010) J Mater Sci 45:3921. doi:10.1007/s10853-010-4457-9
5. Lewandowska M, Kurzydlowski KJ (2008) J Mat Sci 43:7299. doi:10.1007/s10853-008-2810-z
6. Garbacz H, Lewandowska M, Pachla W, Kurzydlowski KJ (2006) J Microscopy 223:272
7. Li X, Liu C, Al-Samman T (2011) Mater Lett 65:1726
8. Steckmeyer A, Radrigo VH, Gentzbittel JM, Rabeau V, Fournier B (2012) J Nucl Mater 426:182
9. Oksiuta Z, Baluc N (2008) J Nucl Mater 374:178
10. Chen Y, Sridharan K, Allen T (2006) Corros Sci 48:2843
11. Mrowec S (1982) Oxidation kinetics and mechanisms. Silesia Publisher, Poland
12. Hoelzer DT, Pint BA, Wright IG (2000) J Nucl Mater 283–287:1306
13. Kaito T, Narita T, Ukai S, Matsuda Y (2004) J Nucl Mater 329–331:1388
14. Takemoto S, Nitta H, Iijima Y, Yamazaki Y (2007) Philosophical Magazine 87(11):1619
15. Ollivier-Leduc A, Giorgi M-L, Balloy D, Guillot J-B (2011) Corros Sci 53:1375
16. Jablonski PD, Alman DE (2008) J Power Sources 180:433
17. Bamba G, Wouters Y, Galerie A, Charlot F, Dellali A (2006) Acta Mater 54:3917
18. Velasco F, Bautista A, González-Centeno A (2009) Corros Sci 51:21
19. McDowell CS, Basu SN (1995) Oxid Met 43(3&4):263